RSC Advances

ROYAL SOCIETY OF CHEMISTRY

www.rsc.org/advances

Cite this: DOI: 10.1039/c0xx00000x

www.rsc.org/xxxxxx

ARTICLE TYPE

Enhancement of Pt-Ru catalytic activity for catalytic wet air oxidation of methylamine *via* tuning Ru surface chemical state and dispersion by Pt addition

Aiying Song [a,b] and Gongxuan Lu [b,*]

Received (in XXX, XXX) Xth XXXXXXXXX 20XX, Accepted Xth XXXXXXXXX 20XX
DOI: 10.1039/b000000x

The enhancement of Pt-Ru catalytic activity for catalytic wet air oxidation (CWAO) of methylamine (MA) was achieved by addition of Pt to Ru catalyst. Pt addition improved catalytic activity of bimetallic catalyst due to tuning Ru surface chemical state and the dispersion of active species. MA was totally mineralized at 200 □ over Pt-Ru catalyst, while temperatures required for total mineralization of MA over Pt and Ru catalysts were 240 and 210 □, respectively. XPS results revealed that addition of Pt could promote the formation of metallic Ru meanwhile TEM and CO chemisorption results confirmed that the addition of Pt promoted the dispersion of active species in the bimetallic catalyst.

Introduction

The release of a great deal of wastewater containing hazardous compounds caused severe environmental problems. Developing efficient technologies for decomposition of pollutants in wastewater in an environmentally friendly way is thus urgent.[1-4] Up to date, many wastewater treating technologies have been developed, such as biological technique,[5] physico-chemical treatment,[6,7] advanced oxidation processes (AOPs), *etc*. Among them, CWAO has attracted great attention for its powerful capabilities in treatment wastewater containing organic pollutants, which is dilute to be incinerated or very concentrated/toxical to be biologically processed.[8-10]

Originated from WAO technique, CWAO was originally developed by Zimmermann and was first industrialized in the late 1950s.[11] By taking advantages of highly reactive oxygen species generated in CWAO process, hazardous compounds can be completely mineralized to CO_2, H_2O and/or N_2 or alternatively to easily biodegradable by-products by controlling reaction conditions.[12, 13] Compared with WAO, the temperature and time CWAO required for mineralization of hazardous compounds were greatly reduced due to the presence of catalysts.[14]

Homogeneous catalysts employed in the CWAO are mainly copper, ferric, and manganese salts. These catalysts are quite efficient since they can fully contact with the pollutants at the molecular level.[15] However, those catalysts are hard to be recycled. In contrast, the heterogeneous catalysts can be conveniently recovered from the reaction medium by simple filtration. So far, many heterogeneous catalysts have been invented, the active components of these catalysts are mainly transition metal oxides and metallic noble metals, such as Co, Ni, Cr, Cu Pt, Ru, Pd, and so on.[16-27] Transition metal oxides are not very selective and stable in CWAO process. Although noble metal-based catalysts are much more expensive than transition metal oxides, their excellent performance and good stability make them receiving much attention in the past decades.[11, 23, 26-28]

The pathways and mechanism of CWAO of organic amine have not been fully understood yet. Qin had proposed that the formation of N_2 was from the reaction between NOH* and NH*, which were generated during ammonia oxidation process.[18] However, Lee indicated that the homogeneous ionic reaction between ammoniac ions and nitrite which was produced by ammonia oxidation was a major route of N_2 formation.[21,29] Pathways and mechanism of nitrogenous organic compounds can be generally summarized as follows: the cleavage of C-N bond giving carboxyl acid and ammonia, and then these intermediates were further oxidized into CO_2 and N_2 as well as other by-products.[30]

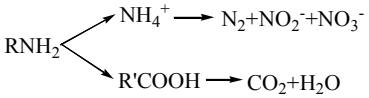

In this work, MA is selected as an objective because it is the simplest organic amine contains both C and N atoms, in the meantime, is a common pollutant presenting in the wastewaters of chemical and pharmaceutical industries.[31,32] In order to treat such a kind of compound, a stable catalyst is necessary. ZrO_2 is used as support because ZrO_2 is resistant to acidic and alkaline media, although it has a disadvantage of low specific surface. Alumina has high specific surface area but unstable under the strong acidic and alkaline conditions. Therefore, a composite support Al_2O_3-ZrO_2 were used in the current CWAO process.[33] In this paper, Pt-Ru, Pt, and Ru catalysts supported Al_2O_3-ZrO_2

were prepared by impregnation method and a detail investigation of their catalytic activities in CWAO of MA was performed. The influences of temperature and liquid hourly space velocity (LHSV) on products distribution were investigated, meanwhile, the pathways and mechanism of degradation of MA was discussed.

Experimental

All reagents were of analytical reagent grade. Commercial alumina (>95%, spherical shape, Kaixin Alumina Co. Ltd., China) was crushed to about 25-45 mesh and subsequently calcined at 600 ℃ for 6 h prior to further use. The alumina particles were modified with zirconia by the impregnation method as follows: 30 g of alumina particles were impregnated into 30 mL aqueous solution containing 5.24 g of $Zr(NO_3)_4{\cdot}5H_2O$ overnight, and then dried at 120℃ for 12 h followed a calcination treatment at 500℃ for 8 h in air. The composition of the Al_2O_3-ZrO_2 support was measured by XRF. The content of Al_2O_3 and ZrO_2 are about 97.81 and 2.18%, respectively.

Pt-Ru/Al_2O_3-ZrO_2, Pt/Al_2O_3-ZrO_2, and Ru/Al_2O_3-ZrO_2 catalysts were also prepared by impregnation method using $H_2PtCl_6{\cdot}6H_2O$ and $RuCl_3{\cdot}xH_2O$ as Pt and Ru precursors, respectively. The total loading amount of metal in three catalysts was fixed at 5 wt.% with respect to Al_2O_3-ZrO_2 and for the preparation of Pt-Ru/Al_2O_3-ZrO_2 catalyst the weight ratio of Pt:Ru kept at 1:1. Briefly, after impregnation of 10 g of modified alumina particles into 10 ml of precursor solution which contains desired amount of H_2PtCl_6 and/or $RuCl_3$, the precursor catalysts were dried at 120 ℃ for 8 h, calcined at 300 ℃ for 8 h, and finally reduced in H_2 flow (40 ml/min) at 300 ℃ for another 8 h. The prepared catalysts were denoted as Pt-Ru, Pt, and Ru for simplicity, respectively.

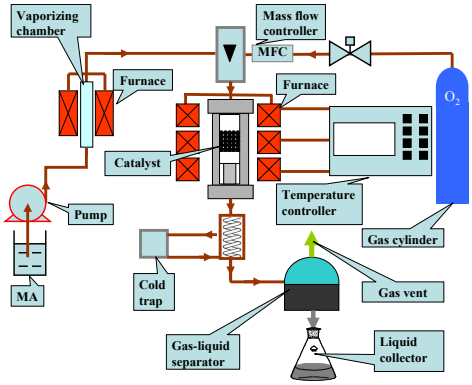

Figure 1 Schematic diagram for CWAO of MA

Catalytic activities of three catalysts were tested in an automated and computer-controlled continuous-flow catalytic evaluation apparatus specialized for heterogenous catalysts (PengXiang Technology Company, Tianjin China), as shown in Figure 1. Briefly, pre-mixed MA solution (2400±120 ppm) was introduced to the vaporizing chamber by using a peristaltic infusion pump (Lab Alliance Series I, USA), after vaporizing, the mixture of MA and steam were merged with oxygen stream (flow rate: 300 ml/min) in a T-joint and then were introduced to the reaction tube which was charged with 10 ml of catalysts. The gas and steam, which passed the catalyst bed and flowed out at the bottom of reactor, were cooled with a cold trap and separated in a gas-liquid separator. The temperature and LHSV were set at each experiment at the desired values. The LHSV was defined as $LHSV=F_{liq}/V_{cat}$, h^{-1}; where F_{liq}=volumetric flow rate of feed solution (ml/h), and V_{cat}=catalyst volume (ml). The reaction liquid at the outlet was periodically extracted from the liquid collector and analyzed for TOC, NH4+, NO2-, and NO3- concentrations. Here, Total Organic Carbon (TOC) is defined as the concentration of total organic compound containing carbon atoms except CO_2, CO and related substances such as carbonate, bicarbonate. Measurement of TOC can provide a rapid and accurate method of determining the concentration of organic contamination, because the amount of organic carbon in wastewater is an indicator of the organic characteristics of the waste effluent. In our work, the value of TOC of input solution and collected liquid after reaction corresponds to the concentration of methylamine because there were no any other organic carbon-containing intermediates formed during the CWAO of MA according to GC/MS analytical results

The elemental analysis of the catalysts was conducted by X-ray fluorescence (XRF) on a Netherlans PANalytical spectrometer. X-ray photoelectron spectroscopy (XPS) measurements were performed on K-Alpha-surface Analysis (Thermon Scientific) using X-ray monochromatization. X-ray diffraction (XRD) patterns of all catalysts were recorded on a Rigaku B/Max-RB diffractometer with a nickel filtrated Cu Kα radiation operated at 40 kV and 40 mA. Transmission electron microscopy (TEM), high-resolution TEM (HRTEM) and elemental mapping images for the catalyst samples were taken by a Tecnai G2-F30 field emission transmission electron microscope operating at accelerating voltage of 300 kV. The specific surface area, total pore volume, and average pore width of the supports and catalysts were determined from the adsorption and desorption isotherms of N_2 at -196℃ using a Micromeritics ASAP 2010 instrument. For GC-MS analysis, a gas chromatography-mass spectrometer (GC-MS) (Agilent 7890 A) with a HP-5MS capillary column (30 m × 0.25 mm × 0.25 mm) coupled with an Agilent 5975 mass spectrometer (Agilent Technologies, Palo Alto, CA) was used. TOC was measured using an Analytik Jena Multi N/C 2100 TOC analyzer (Analytik Jena, Germany). Concentrations of ammonia, nitrite and nitrate ions in the collected liquid were determined using colorimetric method according to Chinese national standard methods (GB/T 5750-2006). The selectivity towards nitrogen (N_2) was computed *via* material balance across 'N' atom. H_2-TPR experiments were carried out by passing a 5% H_2 in Ar stream (flow rate: 15 ml min^{-1}) through the catalysts (50 mg). The temperature increased from 50 to 500 ℃ at a linearly programmed rate of 10 ℃/min. A TCD detector was used to determine the amount of H_2 consumed. CO chemisorption was measured with a Micromeritics ChemiSorb 2750 instrument (Micromeritics, USA). All catalysts were reduced in H_2 diluted with He (10% v/v) flow at 300 ℃ for 120 min. After reduction, catalysts were then flushed at 300 °C for 90 min under He to remove physisorbed hydrogen. The catalysts were subsequently cooled under the same He stream. The chemisorbed CO was analyzed at 35 °C.

Results and discussion

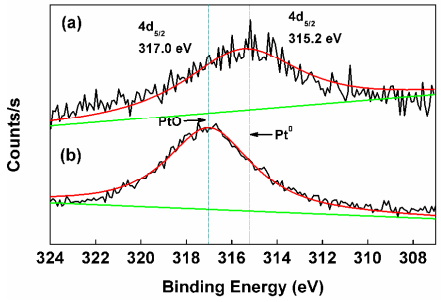

Figure 2 XPS Pt $4d_{5/2}$ spectra for (a) Pt-Ru and (b) Pt catalysts.

The surface chemical states of metal NPs in Pt-Ru, Pt, and Ru catalysts were investigated with XPS technique. The most intensive photoemission lines of Pt $4f_{7/2}$ and Ru $3d_{5/2}$ levels are overlapped with Al 2p and C 1s lines from alumina support and carbon contaminants, respectively. Therefore the Pt and Ru surface species were investigated by analyzing the Pt $4d_{5/2}$ and Ru $3p_{3/2}$ lines. Figure 2 shows the Pt $4d_{5/2}$ XPS spectra of Pt-Ru and Pt catalysts. The Pt $4d_{5/2}$ peak centered at 315.2 eV in Pt-Ru belongs to Pt^0 species while the Pt $4d_{5/2}$ peak at 317.0 eV in Pt catalyst is assigned to Pt^{2+} species.[34] The XPS results indicate the presence of Pt metal in the Pt-Ru catalyst while the Pt oxide in the Pt catalyst, which reveals that the Pt precursor can be more easily converted into metallic Pt in the presence of Ru.

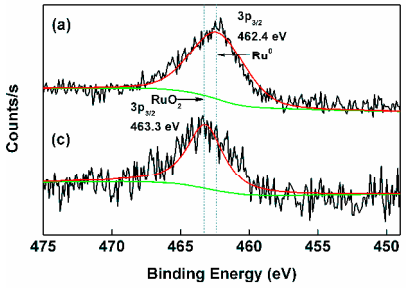

Figure 3 XPS Ru $3p_{3/2}$ spectra for (a) Pt-Ru and (c) Ru catalysts.

The similar results can be observed from the XPS spectra of Ru based catalysts (Figure 3). The binding energy Ru $3p_{3/2}$ (462.4 eV) in Pt-Ru catalyst indicates the presence of metallic Ru while the binding energy Ru $3p_{3/2}$ (463.3 eV) in Ru catalyst reveals the presence of Ru oxides.[35] This effect is similar to that of Ru-promoted reduction of Pt precursor in Pt-Ru catalyst, suggesting that co-existence of Pt and Ru favours the formation of metallic species in the bimetallic catalyst. The presence of metallic species may contribute to the enhancement of catalytic activity of Pt-Ru for CWAO of MA because the catalytic activity of metallic Pt and Ru are higher than that of their oxides and this issue will be further discussed in our future work.

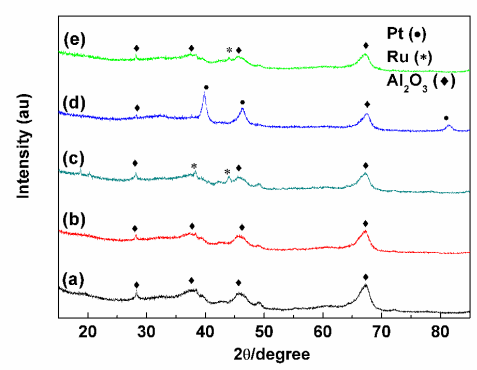

Figure 4 X-ray diffraction patterns of (a) Al_2O_3, (b) Al_2O_3-ZrO_2, (c) Pt-Ru, (d) Pt, and (e) Ru.

Figure 4 (a-e) shows X-ray diffraction (XRD) patterns of Al_2O_3, Al_2O_3-ZrO_2, Pt-Ru, Pt, and Ru catalysts. The peaks in Figure 4a of patterns at 19.5°, 39.6°, 46.0°, 60.6°, and 67.3° can be assigned to the cubic alumina structures (411), (222), (400), (511), and (440). No obvious diffraction peaks of crystalline ZrO_2 can be observed in XRD patterns of Al_2O_3-ZrO_2 (Figure 4b), which is probably due to either small particle size or low content of ZrO_2.

The crystalline structure of metal in Pt catalyst revealed by XRD pattern shows three typical obvious diffraction peaks at around 40.0°, 46.2°, and 81.3°, which can be indexed to (111), (200), and (311) planes of a face-centered cubic *(fcc)* structure for Pt (Figure 4d). On the contrary, in the XRD analysis for Ru catalyst that there is only a diffuse diffraction peak at 2θ=44.0°, corresponding to (100) plane of a primitive hexagonal close-packed (*hcp*) crystalline Ru (Figure 4e).

In case of Pt-Ru catalyst, only typical diffraction peaks at 38.4° and 44.0° corresponding to (101) and (100) planes of *hcp* crystalline Ru can be observed. Whereas no Pt^0 species diffraction peaks appear probably due to the intensities of its reflections are weaker than those of Ru species (Figure 4c). These analytical results suggest that Pt and Ru components in the bimetallic catalyst did not form alloy and maybe existed as separate bimetal architectures. Similar experimental results had been observed by Zhou *et al.* during preparation of Pt-Ru/AlOOH catalyst by using $H_2PtCl_6{\cdot}6H_2O$ and $RuCl_3{\cdot}xH_2O$ as precursors by co-impregnation and hydrothermo reduction methods.[36]

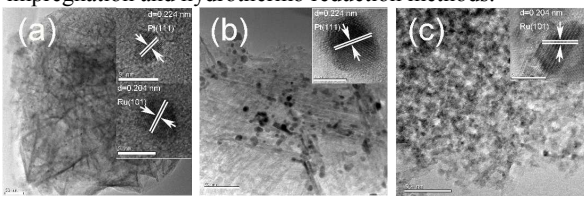

Figure 5 TEM images of Pt-Ru, Pt, and Ru catalysts a, b, and c. The insets in panels a, b, and c are HRTEM of deposited Pt and/or Ru NPs, respectively.

In order to further explore crystalline structures and dispersion of metal NPs over Pt-Ru, Pt, and Ru catalysts, the TEM images were taken. Figure 5a, b, and c show the low-magnification TEM images. As observed from these images, the supported metal NPs in all catalysts are well-dispersed throughout support substrate with a nearly spherical morphology, however, comparing with Figures 5a, b, and c, it is clear that the small black metal particles are more uniformly dispersed onto the support in bimetallic catalyst than those in the monometallic ones.

The HRTEM images of Pt-Ru catalyst (insets in Figure 5a) shows two set of lattice fingers with *d*-spacing of 0.224 and 0.204 nm, which can be respectively indexed to (111) plane of *fcc* Pt and (101) plane of *hcp* Ru, reconforming that Pt and Ru in bimetallic catalyst exists as separate bimetal architectures. For Pt and Ru catalysts, their HRTEM images (insets in Figures 5b and c) show that *d*-spacings of adjacent fringe are 0.224 and 0.204 nm, corresponding to the (111) and (101) crystalline planes of *fcc* Pt and *hcp* Ru lattice, respectively. These results are in accordance with the XRD results presented above.

In order to confirm the presence of metal elements, three catalysts were characterized by elemental mapping and energy dispersive X-ray spectrometry (EDX) measurements. As shown in Figure S1, the elemental mapping images of three catalysts obviously demonstrate that the distributions of the elements Pt and/or Ru. Clearly, the elemental distribution profiles of Pt and Ru indicate that Pt and Ru NPs are well distributed onto the support. In Figure S2, EDX results show the corresponding peaks of C, O, Al, Cu, Zr, Pt, and/or Ru of different catalysts.

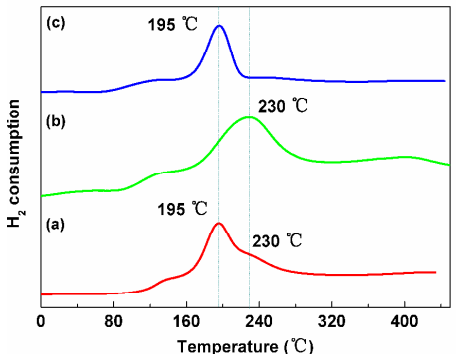

Figure 6 Temperature programmed reduction profiles of (a) Pt-Ru, (b) Pt, and (c) Ru catalysts.

H_2-TPR is conducted over three catalysts to understand the reduction behaviors of Pt and/or Ru oxides in the calcined catalysts, as shown in Figure 6. The main reduction peak for Pt catalyst presents at 230 ℃, which should be attributed to the reduction of PtO_x and/or PtO_xCl_y species on the support, and there is no interaction between those species and support.[37] The broad peak of Pt reduction means that Pt particle size distributed in a large range and this speculation can be confirmed by its TEM analysis (Figure 5b). This phenomenon usually occurred on Pt/Al_2O_3 catalyst prepared by impregnation, in which the particle size was difficult to be delicately controlled.

For Ru catalyst, only a sharp reduction peak appears at about 195 ℃, which indicates precursor $RuCl_3$ was completely transformed into RuO_x after calcination in air.[38,39] In case of Pt-Ru catalyst, the peak maximum appears at 195 ℃ (ascribed to RuO_x) with a shoulder at 230 ℃ (ascribed to PtO_x and/or PtO_xCl_y species). TPR results confirm that there is no alloy formation between Pt and Ru.

Table 1 Textural characterization of support and Pt-Ru, Pt, and Ru catalysts with the dispersion of active species in all catalysts.

Catalyst	BET (m^2/g)	Pore volume (cm^3/g)	Pore Size (nm)	Dispersion (%)
Al_2O_3	162	0.49	12	-
Al_2O_3-ZrO_2	163	0.42	10	-
Pt-Ru	158	0.49	12	38
Pt	156	0.49	13	26
Ru	152	0.46	12	12

The surface area, pore volumes, pore sizes of the support, Pt-Ru, Pt, and Ru catalysts with the dispersion of active species in this study are listed in Table 1. The surface area of Al_2O_3 was hardly changed after modification by ZrO_2. But there was a slight loss of surface area for the as-prepared catalysts while the values of the pore volumes and diameters nearly kept constant, which indicated that precious metal NPs were successfully supported onto Al_2O_3-ZrO_2 and the textural properties of support remained unchanged after impregnation. The Pt-Ru and Pt catalysts have dispersions values of 38 and 26%, respectively. However, a poor dispersion (12%) was observed for Ru catalyst. From Table 1 it appears that the combined dispersion of Pt-Ru (38%) matches with the summation of the individual dispersions of Pt (26%) and Ru (12%). This also confirms that there is no interaction between Pt and Ru in the bimetallic catalyst.

In order to investigate the effects of reaction temperature on the catalytic activities of Pt-Ru, Pt, and Ru catalysts in CWAO of MA, the TOC (total organic carbon, defined as the concentration of total organic compound containing carbon atoms except CO_2, CO and related substances), N-containing compounds yield such as NH_4^+, NO_2^-, and NO_3^- were directly measured and N_2 was computed *via* material balance across 'N' atom. TOC conversion (refer to activity) and selectivity of nitrogen species (refer to selectivity) are expressed as the following ratio:

Activity (%) = $(1\text{-}TOC_{determined}/TOC_{ini})\times100$

Selectivity (%) = $(molN_{lq\text{-}class}/mol_{MAini})\times100$ or

Selectivity (%) = $(2\times molN_2/mol_{MAini})\times100$

where the "molNlq-class" means the total amount of N-contained compounds detected in the collected liquid after reaction, including NH_4^+, NO_2^-, and NO_3^-.

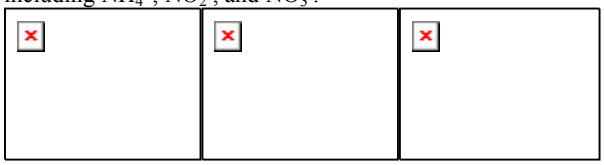

Figure 7 Influence of the temperature on the TOC conversion over (a) Pt-Ru, (b) Pt, and (c) Ru catalysts.

Figure 7 shows the variation of TOC conversion with temperature over Pt-Ru, Pt, and Ru catalysts. It can be seen that reaction temperatures have great influence on catalyst's activity for oxidation of MA. Typically Pt-Ru and Ru catalysts have higher catalytic activity than Pt catalyst for CWAO of MA in examined temperature ranges. For Pt catalyst, MA was completely mineralized until at 240 ℃ (Figure 7b), where the TOC conversion reached 100%; however, temperatures required to fully decompose MA were only 200 and 210 ℃ over Pt-Ru and Ru catalysts (Figure 7a and c), respectively. These results suggested that Pt catalyst was not very efficient in degradation of MA, though Pt was more active than Ru in ammonia eliminating[1], probably due to Pt has difficulties in cleaving C-N bonds of MA. Pt-Ru catalyst, as expected, demonstrated the highest catalytic activity among three catalysts. Based on XPS and CO chemisorption analysis, it comes to the conclusion that the decrease in temperature for obtaining high activity over Pt-Ru

catalyst benefits from the presence of metallic species and the high dispersion of active species in the bimetallic catalyst. In Pt-Ru catalyst, Ru is a primarily active component in C-N bond cleavage for production of NH_3 and N_2, whereas Pt serves as the promoter to formation of metallic species and enhancement of dispersion of active species in bimetallic catalyst. As a result, Pt-Ru catalyst displayed an excellent activity and the catalytic activity of three catalysts for the CWAO of MA in term of TOC conversion, followed the order of Pt-Ru>Ru>Pt.

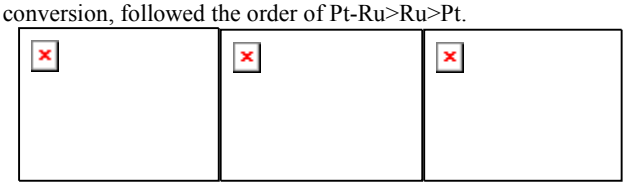

Figure 8 Influence of the temperature on the N_2 selectivity over (a) Pt-Ru, (b) Pt, and (c) Ru catalysts.

Figure 8 shows the MA conversion to N_2 as a function of temperature over three catalysts. It can be seen from results over Pt-Ru catalyst in Figure 8 that the C-N bond cleavage only leads to formation of amount of ammoniac ions at low temperature (Figure S3) and no N_2 produced over Pt-Ru and Pt catalysts. Whereas there were small amounts of N_2 still produced over Ru catalyst at low temperature, which indicated that Ru catalyst has excellent selectivity toward N_2 in this work. These experimental results revealed that CWAO of MA over three catalysts probably followed two different pathways, that is, over Pt based catalysts, C-N bond of MA was firstly cleaved to form NH_3 and then to N_2 by further oxidation of NH_3, but C-N bond cleavage lead to both NH_3 and N_2 simultaneously over Ru catalyst. With temperature increasing, ammonia yield reduced after reaching maximum while N_2 yields constantly increased and eventually approached to ~100%. In all experiments, the concentration of NO_2^- and NO_3^- are no more than 3.84 and 2.4 ppm, respectively (≤1.6 and ≤1.0 ‰, as shown in Figures S4 and S5).

Interestingly, as shown in Figures 7 and 8, temperature hysteresis can be observed in TOC conversion and selectivity toward N_2 over three catalysts. This phenomenon can be also observed in catalytic oxidation of CO over Cu/YSZ (yttria-stabilized zirconia) and Cu/γ-alumina catalysts.[40] For example, over Pt-Ru catalyst, the TOC conversion reduced from 87.0 to 69.7% as temperature decreased from 180 to 170℃, while it was only possible to get the same TOC conversion when temperature increased from 178 to 185℃ during heating direction (Figure 7a). Based on the hysteresis phenomena presented in Figures 7 and 8, we tentatively propose that the mechanism of CWAO of MA follows a chemisorption-type mechanism which is similar to that of catalytic oxidation of CO reaction. A possible explanation of hysteresis phenomena observed in this study can be described as following: the temperature, as well known, always controls and determines the adsorption strength of active sites towards reactants. In this experiment, the adsorbed oxygen molecule may not be desorbed from catalysts' surface during cooling until the temperature decreased to a certain one for a long time and the amount of adsorbed oxygen molecules was proportional to concentration of activated oxygen species which directly reacted with MA molecules to mainly produce CO_2 and N_2, thus TOC conversion and nitrogen selectivity in cooling were higher than those in heating.

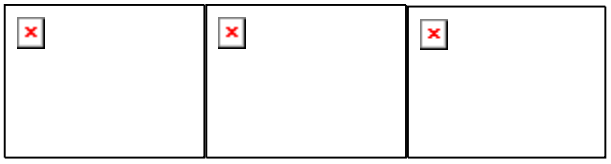

Figure 9 Influence of LHSV on the TOC conversion over (a) Pt-Ru, (b) Pt, and (c) Ru catalysts.

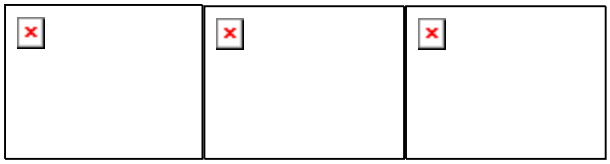

Figure 10 Influence of LHSV on the N_2 selectivity over (a) Pt-Ru, (b) Pt, and (c) Ru catalysts.

Results in Figures 9, 10, S6, S7, and S8 show that the LHSV greatly influenced TOC conversion and selectivity towards N_2, NH_4^+, NO_2^-, and NO_3^- products (refer to N-form products) over three catalyts in examined LHSV range (0.6-5.4 h^{-1}), respectively. As expected, the higher liquid LHSV and lower temperature, the lower conversion of TOC and N_2 selectivity (Figures 9 and 10) were obtained in experiment, indicating the catalytic activities of all catalysts were affected by both temperature and LHSV due to which greatly affect the ratio of MA and activated oxygen species. At high LHSV and low temperature, there was no nitrogen formed and only a large amount of ammonia ions was produced over Pt-Ru catalyst, while both NH_4^+ and N_2 were formed over Ru catalyst (Figures 10 and S6). These experimental results reconfirmed that Ru has better selectivity toward N_2 than Pt based catalysts and MA was decomposed according to two different pathways over three catalysts. In addition, high temperature and/or low LHSV seems to favour formation of nitrite and nitrate by-products (Figures S7 and S8).

In order to assess the stability of catalysts, endurance tests were performed at 200, 240, 210 ℃ and liquid hourly space velocity (h^{-1}, LHSV) of 3.0 h^{-1} for Pt-Ru, Pt, and Ru catalysts for 300 h, respectively. As a result, the TOC conversion and nitrogen selectivity basically maintained at about 100% during the whole time on stream, which indicates that all catalysts exhibited rather stable catalytic behaviours during 300 h of time on stream.

In order to explore the degradation pathway of MA in the process of catalytic oxidation, GC-MS was applied to identify the hydroxyl amine and organic intermediates in the collected liquid and the condensate. Surprisingly, analytical results show that there were no hydroxyl amine and organic intermediates formed during the CWAO of MA process. On the basis of inorganic product distribution in the collected liquids and the condensate, we proposed a reaction pathway for the degradation of MA on CWAO, as given in Scheme 1. it was concluded that after scission of C-N bond, CH_3 fragment was fully converted into CO_2 while NH_2 fragment was oxidized into N_2 and/or NH_4^+, NO_2^-, NO_3^- and NH_4^+ can be further oxidized into N_2, NO_2^-, and NO_3^-. It should be noted that CO_2 and N_2 are the predominant products during MA oxidation reaction.

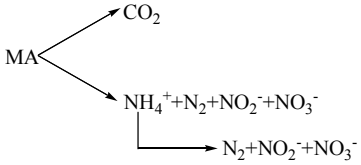

Scheme 1 MA oxidation pathways.

Conclusions

XPS studies indicate that the co-existence of Pt and Ru favours the formation of metallic components while TEM and CO chemisorption results confirm the promotion of the dispersion of active species in the bimetallic catalyst, which may contribute to enhancement of catalytic activity of Pt-Ru for CWAO of MA. The TOC conversion and selectivity toward N-form products at different temperatures and LHSV on different catalysts revealed that Pt catalyst was not very efficient in C-N cleavage whereas Ru was capable of both C-N cleavage and ammonia eliminating. Only trace nitrite and nitrate ions were formed during CWAO process, so the experimental procedures employed in this work may provide a useful clue to avoiding formation of these undesired by-products in CWAO of nitrogen-containing compounds.

Acknowledgments

We acknowledge the financial supports of the National Science Foundation of China (Grant Nos. 21373245, 21173242), 973 and 863 Programs of Department of Sciences and Technology of China (Grant Nos. 2013CB632404, 2012AA051501, 2009CB22003), and the Project Support of Gansu Provincial Science & Technology Department (1304FKCA085).

Notes and references

a State Key Laboratory for Oxo Synthesis and Selective Oxidation Lanzhou Institute of Chemical Physics, University of Chinese Academy of Sciences, Lanzhou 730000, P. R. China. E-mail: gxlu@lzb.ac.cn; Fax: (+86) 931 4968178

b Chemical Physics Laboratory of Gansu Provincial Center for Disease Control and Prevention, Lanzhou 730020, P. R. China

1 J. Barbier, L. Oliviero, B. Renard, D. Duprez. *Catal. Today*, 2002, **75**, 29.
2 C. Aguilar, R. Garcia, G. Soto-Garrido, R. Arraigada. *Top. Catal*., 2005, **33**, 201.
3 Y. Xu, X. Li, X. Cheng, D. Sun. *Environ. Sci. Technol.*, 2012, **46**, 2856.
4 R. Levi, M. Milman, M. V. Landau, A. Brenner, M. Herskowitz. *Environ. Sci. Technol.*, 2008, **42**, 5165.
5 C. S. Tripathi, D. G. Allen. *Water Res*., 1999, **33**, 836.
6 A. B. Bjerre, E. Soerensen. *Ind. Eng. Chem. Res*., 1992, **31**, 1574.
7 C. J. Martino, P. E. Savage. *Ind. Eng. Chem. Res*., 1997, **36**, 1385.
8 D. Ghosh, K. G. Bhattacharyya. *Appl. Clay Sci*., 2002, **20**, 295.
9 L. Oliviero, J. Barbier, Duprez, D. *Appl. Catal. B*, 2003, **40**, 163.
10 E. Castillejos-Lopeza, A. Maroto-Valientea, D. M. Nevskaiaa, V. Munoza, Rodriguez-Ramos, I. A. Guerrero-Ruiz. *Catal. Today*, 2009, **143**, 355.
11 Zimmerman, F. J. U.S. 1950, Patent No. 2, 665,249.
12 D. K Lee, D. S. Kim, *Catal. Today* 2000, **63**, 249.
13 C. M. Hung. *J. Hazard. Mater*. 2010, **180**, 561.
14 H. T. Gomes, B. F. Machado, A. Ribeiro, I. Moreira, M. Rosario, A. M. T. Silva, J. L. Figueiredo, J. L. Fari. *J. Hazard. Mater*., 2008, **159**, 420.
15 F. Arena, C. Italiano, A. Raneri, C. Saja. *Appl. Catal. B*, 2010, **99**, 321.
16 N. Okada, Y. Nakanishi, Y. Harada, 1977, United States Patent 4 141 828.
17 H. T. Gomes, P. Selvam, Dapurkar, S. E. Figueiredo, J. L. Faria, J. L. *Micropor. Mesopor. Mat*., 2005, **86**, 287.
18 J. Qin, K. Aika. *Appl. Catal B*, 1998, **16**, 261.
19 S. K. Kim, S. K. Ihm. *Top. Catal*., 2005, **33**, 171.
20 J. Taguchi, T. Okuhara. *Appl. Catal A: Gen*, 2000, **194-195**, 89.
21 D. K. Lee. *Environ. Sci. Technol*., 2003, **37**, 5745.
22 S. Kaewpuang-Ngam, K. Inazu, K. I. Aika. *Res. Chem. Intermed.*, 2002, **28**, 471.
23 G. Sun, A. Xu, Y. He, M. Yang, H. Du, C. Sun. *J Hazard. Mater*., 2008, **156**, 420.
24 N. D. Tran, M. Besson, C. Descorme, K. Fajerwerg, C. Louis. *Catal. Commun.*, 2011, **16**, 98.
25 F. Nunez, D. Gloria, F. Tzompantzi, J. Navarrete. *Ind. Eng. Chem. Res*., 2011, **50**, 2495.
26 J. Jr. Barbier, L. Oliviero, B. Renard, D. Duprez. *Top. Catal*., 2005, **33**, 77.
27 S. Imamura, I. Fukuda, S. Ishida. *Ind. Eng. Chem. Res*., 1988, **27**, 718
28 D. Lee; J. Cho, W. Yoon, *Chemosphere*, 2005, **61**, 573.
29 G. R. Reddy, V. V. Mahajani. *Ind. Eng. Chem. Res*., 2005, **44**, 7320.
30 N. Grosjean, C. Descorme, M. Besson. *Appl. Catal B*, 2010, **97**, 276.
31 M. Abalos, J. M. Bayona, F.Ventura. *Anal. Chem.,* 1999, **71**, 3531.
32 F. Sacher, S. Lenz, H. J. Brauch, *J. Chromatogr. A,* 1997, **764**, 85.
33 F. Núñez, G. D. Angel, F. Tzompantzi, J. Navarrete. *Ind. Eng. Chem. Res.,* 2011, **50**, 2495.
34 G. Corro, J.L.G. Fierro, V.C. Odilon, *Catal. Commun*., 2003, **4**, 371.
35 A.S. Aricò, V. Baglio, A. Di Blasi, E. Modica, P.L. Antonucci, V. Antonucci, *J Electroanal. Chem*., 2003, **557**, 167.
36 Y. F. Zhou, H. Y. Fu, R. X. Li, H. Chen, X. J. Li, *Catal. Commun*. 2009, **11**, 137.
37 H. C. Yao, M. Sieg, *J Catal*., 1979, **59**, 365.
38 P. G. J. Koopman, A. P. G. Kieboom, H. V. Bekkum, *J. Catal.*, 1981, **69**, 172.
39 P. Betancourt, A. Rives, R. Hubaut, C. E. Scott, J. Goldwasser, *J. Appl. Catal. A*, 1998, **170**, 307.
40 W. P. Dow, Y. P. Wang, T. J. Huang, *J Catal*. 1996, **160**, 171.

Graphical abstract

Formatted: Font color: Auto

Enhancement of Pt-Ru catalytic activity for catalytic wet air oxidation of methylamine *via* tuning Ru surface chemical state and dispersion by Pt addition

In this work, Ru-Pt, Pt and Ru catalysts supported on the alumina modified with zirconia were prepared by impregnation methods. The as-prepared catalysts were employed in the catalytic wet air oxidation (CWAO) of methylamine (MA). By correlating catalytic activity and structure of catalyst samples, we found that Pt addition can improve catalytic activity of Ru catalyst by tuning Ru surface chemical state and the dispersion of active species in the bimetallic catalyst. The temperature-dependent hysteresis over TOC conversion and N_2 selectivity revealed that the CWAO of MA follows a chemisorption mechanism.